Computer Methods and Programs in Biomedicine 240 (2023) 107678

Contents lists available at ScienceDirect

Computer Methods and Programs in Biomedicine

journal homepage: www.elsevier.com/locate/cmpb

A novel epileptic seizure prediction method based on synchroextracting transform and 1-dimensional convolutional neural network

Jee Sook Ra*, Tianning Li, YanLi

School of Mathematics, Physics and Computing, University of Southern Queensland, Toowoomba, QLD 4350, Australia

ARTICLE INFO

Article history:
Received 23 December 2022
Revised 7 June 2023
Accepted 12 June 2023

Keywords:
EEG analysis
Synchroextracting transform (SET)
Singular value decomposition (SVD)
1-dimensional convolutional neural network (1D-CNN)
Epileptic seizure prediction

ABSTRACT

Background and objective: Epilepsy is a serious brain disorder affecting more than 50 million people worldwide. If epileptic seizures can be predicted in advance, patients can take measures to avoid unfortunate consequences. Important approaches for epileptic seizure predictions are often signal transformation and classification using electroencephalography (EEG) signals. A time-frequency (TF) transformation, such as the short-term Fourier transform (STFT), has been widely used over many years but curtailed by the Heisenberg uncertainty principle. This research focuses on decomposing epileptic EEG signals with a higher resolution so that an epileptic seizure can be predicted accurately before its episodes.
Methods: This study applies a synchroextracting transformation (SET) and singular value decomposition (SET-SVD) to improve the time-frequency resolution. The SET is a more energy-concentrated TF representation than classical TF analysis methods.
Results: The pre-seizure classification method employing a 1-dimensional convolutional neural network (1D-CNN) reached an accuracy of 99.71% (the CHB-MIT database) and 100% (the Bonn University database). The experiments on the CHB-MIT show that the accuracy, sensitivity and specificity from the SET-SVD method, compared with the results of the STFT, are increased by 8.12%, 6.24% and 13.91%, respectively. In addition, a multi-layer perceptron (MLP) was also used as a classifier. Its experimental results also show that the SET-SVD generates a higher accuracy, sensitivity and specificity by 5.0%, 2.41% and 11.42% than the STFT, respectively.
Conclusions: The results of two classification methods (the MLP and 1D-CNN) show that the SET-SVD has the capacity to extract more accurate information than the STFT. The 1D-CNN model is suitable for a fast and accurate patient-specific EEG classification.

1. Introduction

Epilepsy is characterized by aberrant brain activity that results in seizures or episodes of abnormal behaviors, sensations, and occasionally loss of consciousness. If epileptic seizures can be predicted in advance, unfortunate consequences for the patient can be mitigated. One important area of seizure prediction research is feature extraction and classification based on electroencephalography (EEG) signals, which are various electrical activities measured across the scalp using small metal discs (electrodes). While some EEG-based seizure prediction algorithms are patient-independent, this study customizes experimental methods to individual patients' EEG signals (patient-dependent).

Signal processing is employed in many applications to provide underlying information on specific problems so that useful features can be extracted. There has been intensive research on the time domain, frequency domain and time-frequency domain for EEG signal analysis. Time domain analysis often is not sufficient for obtaining all useful information. Frequency domain analysis generates only spectral information about the signal but not the time-domain information at the same time. Therefore, EEG data in the time domain are often transformed into the time-frequency (TF) domain using various different methods, such as short-time Fourier transform (STFT) [1], wavelet analysis (WA) [2,3] or multiresolution Fourier transform (MFT) [4]. However, despite decades of development, the TF analysis method has been constrained by the Heisen-

* Corresponding author.
E-mail addresses: jee.ra@usq.edu.au (J.S. Ra), Tianning.Li@usq.edu.au (T. Li), Yan.Li@usq.edu.au (YanLi).

https://doi.org/10.1016/j.cmpb.2023.107678

Table 1
Overview of the reviewed articles.

Author	Methods	Dataset	Accuracy	Sensitivity	Specificity
Khalilpour et al. (2020) [16]	Raw EEG data, 1-D CNN	CHB-MIT [1]	97%	98.5%	98.5%
Prathaban & Balasubramanian (2021) [17]	Sparsity based EEG reconstruction, 3-D CNN	CHB-MIT, SRM [2], NINC [3]	98%	99%	90%
Wang et al. (2021) [18]	STFT, 3-D CNN	CHB-MIT	80.5%	85.8%	75.1%
Truong et al. (2017) [12]	STFT, 2-D CNN	CHB-MIT, Freiburg [4], KSPC [5]	NA	NA	81.4%
Chen and Parhi (2021) [13]	STFT, 2-D CNN	AESPC [6]	NA	NA	82%
Sun et al. (2021) [14]	STFT, Channel attention dual-input CNN	CHB-MIT	NA	97.1%	95.6%
Shahbazi and Aghajan [19]	STFT, 2-D CNN + LSTM	CHB-MIT	NA	98.2%	NA

[1] Children's Hospital Boston and the Massachusetts Institute of Technology Scalp EEG Dataset.
[2] Private SRM dataset.
[3] Neonatal EEG recordings with seizure annotations of Neonatal Intensive Care Unit acquired from Helsinki University Hospital.
[4] Freiburg iEEG dataset.
[5] Kaggle seizure prediction competition dataset.
[6] The American Epilepsy Society Prediction Challenge dataset.

berg uncertainty principle [5,6] or unanticipated cross-terms [7]. Since TF-based analysis methods use wide bandwidth in the TF domain, the energy of the generated TF representation smears heavily according to the Heisenberg uncertainty principle. In addition, when there are many components in the input signal, which is similar to frequency beats in time, a cross-term occurs. As a result, TF-based analysis methods experience a low TF resolution [5,8]. In recent years, many signal transformation methods were developed to overcome those issues, which are instrumental in decrypting patterns from epileptic EEG signals. One of them is synchroextracting transform (SET) [9], the novel TF analysis method which improves the energy concentration in the TF representation [9]. Meanwhile, one of the restraints of applying the SET is generating many sub-signals that can cause significant time consumption and computational cost or sometimes inhibit accurate classification performance due to many dimensions. After a SET decomposition, the singular value decomposition (SVD) is applied to minimize a large number of sub-signals without losing the crucial information in the SET preserves (SET-SVD). The last step of this study is the classification of the pre-ictal period and normal period using two types of neural networks (NNs), multi-layer perceptron (MLP) and 1-dimensional convolutional neural network (1D-CNN), to compare with the performances of the SET and STFT resolutions. A convolutional neural network (CNN) is a common term used to describe a 2-dimensional CNN (2D-CNN) used for image classification and signal processing, given that the kernel moves along the data in two dimensions. In many situations, however, a 2D-CNN may not be feasible for 1-dimensional signals (such as time series signals), particularly if the training data are limited or time-corresponding. In this study, a 1D-CNN is used to reduce processing time and accomplish more effective classification, and the outcomes are compared to those of a multi-layer perceptron (MLP). The following is a summary of the major contributions of this study:

- With the proposed method, pre-ictal signals in epileptic EEG signals can be accurately detected.
- The proposed method reduces the classification computational time. Real-time seizure prediction can, therefore, be enabled.
- A better signal transformation method can be discovered by contrasting different signal transformation methods with the same classification algorithms. Nevertheless, this procedure takes a considerable amount of time and effort, and this study can be used as a benchmark reference for different types of signal analysis.

The remainder of this paper is arranged as follows. In Section 2, related works are discussed. Section 3 presents the details of the datasets used in this paper, data preprocessing, the proposed techniques for signal transformation (SET, STFT and SVD) and classification (MLP and 1D-CNN). Section 4 explains the experimental setups and results. Section 5 discusses the findings of this research. Finally, the conclusions of this study are drawn in Section 6.

2. Related works

The STFT has been widely used for EEG signal analyses as it is simple and adaptive to be implemented [10]. For example, Gorur et al. (2002) achieved an accuracy of 88.7% by applying a STFT and neural network (NN) method for the sleep spindles detection [11]. Some research applying the STFT for seizure prediction, especially using a CNN, has shown desirable results. Truong et al. (2017) applied a STFT with a CNN for seizure prediction [12] and reached a sensitivity of 81.4%. Chen and Parhi (2021) also used a STFT and a CNN and achieved an overall sensitivity of 82% [13]. A STFT with a channel attention dual-input CNN showed a better sensitivity of 95.6% [14]. On the other hand, so far, no study has applied the SET for seizure prediction yet. Kiranyaz et al. (2015) developed the first adaptable 1-dimensional CNN (1D-CNN) model for a fast and accurate patient-specific electrocardiogram (ECG) classification, and achieved 99% of accuracy [15]. Khalilpour et al. (2020) used a seven-layer 1D-CNN to detect pre-ictal and normal periods in the brain signals, where the performance was evaluated in terms of accuracy, specificity, and sensitivity which resulted in 97%, 98.47%, and 98.5%, respectively. Table 1 summarizes the reviewed articles that employed CNNs or STFT for the prediction of epileptic seizures (detection of pre-ictal signals).

3. Methodology

This study aims to find an excellent accurate epileptic seizure prediction method. Comparison is a way to justify that our method is optimum. As a result, this comparison may help establish a less complex seizure prediction system with a higher resolution of EEG signal transformation. In this research, the raw EEG signals without noise removal are converted using the SET and STFT respectively, and the dimensionality of the results obtained by the SET is reduced by a SVD. The decomposed and chosen values of the signals are then classified using two types of neural networks, the MLP and 1D-CNN, and their classification performances are then compared. The fundamental procedure of the proposed method is illustrated in Fig. 1.

3.1. Experimental data

Long-term annotated data are required for the development of seizure prediction algorithms. Hospitals and research institutions have created open-access databases, and two well-known epilepsy datasets (the Bonn University (Bonn) database and the Children's Hospital Boston-Massachusetts Institute of Technology (CHB-MIT) scalp EEG database) are accessible online. This study evaluates the

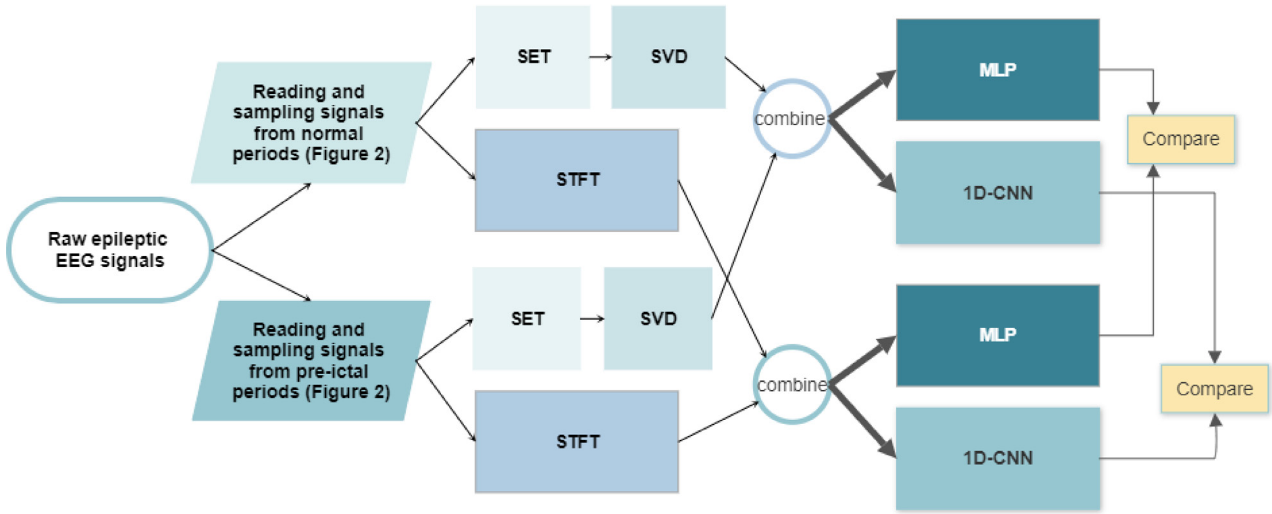

Fig. 1. The main processing diagram of the proposed methodology.

Table 2
The characteristics of each patient and the patient's information data used in this paper [20].

Recording number	Patient ID	Gender	Age	Number of seizures	Length of records (Hours)
chb01	1-1	F	11	7	45.00
chb02	2	M	11	3	39.57
chb03	3	F	14	7	57.87
chb04	4	M	22	4	154.41
chb05	5	F	7	5	38.09
chb06	6	F	1.5	10	89.25
chb07	7	F	14.5	3	67.23
chb08	8	M	3.5	5	26.38
chb09	9	F	10	4	65.92
chb10	10	M	3	7	72.49
chb11	11	F	12	3	73.30
chb12	12	F	2	40	NA[1]
chb14	14	F	9	8	41.50
chb15	15	M	16	20	62.29
chb16	16	F	7	10	17.03
chb17	17	F	12	3	34.11
chb18	18	F	18	6	62.85
chb19	19	F	19	3	61.58
chb20	20	F	6	8	41.43
chb21	1-2	F	13	4	55.71
chb22	21	F	9	3	75.93
chb23	22	F	6	7	70.90

[1] Not available. Not specified.

proposed method on the two publicly available databases (Bonn and CHB-MIT). The information about the two databases is provided below.

3.1.1. CHB-MIT database

EEG recordings of pediatric patients with uncontrollable seizures are available in the CHB-MIT database [16]. Twenty-four recordings were collected from 23 patients (5 males (ages 3–22) and 17 females (ages 1.5–19); information for Patient ID 23 is not specified). Recordings chb01 (Patient ID 1-1) and chb01 (Patient ID 1-2) were obtained from the same female patient. A single recording is represented by nine to forty-two continuous *.edf* files (chb01, chb02, or others). Patients were monitored for up to several days after stopping anti-seizure medication in order to describe their epileptic seizures and determine whether they were a good candidate for surgery. In this study, 22 out of 24 recordings are analyzed. Two recordings (chb13 and chb24) are excluded from this study because they are unsuitable for experimentation due to frequent channel changes during the EEG recording; Table 2 provides information about 22 recordings.

3.1.2. Bonn database

This EEG database is publicly available and provided by the University of Bonn as acquired by Andrzejak et al. [21]. It consists of five datasets: A, B, C, D, and E. Each dataset consists of 100 single-channel EEG files with a duration of 23.6 seconds and a total of 4097 samples as shown in Table 3. 12-bit analogue-to-digital converters sampling at 173.61 Hz were used. The EEG database consists of 5 classes x 100 files x 4097 data points (23.6 seconds).

3.2. Epileptic EEG data pre-processing

Four stages are commonly used to categorize epileptic EEG signals: normal, pre-ictal, ictal, and post-ictal periods (Fig. 2). To avoid a relatively high ratio of normal period data in the classification, the normal to pre-ictal training/testing data ratio is capped at 10:1 [20]. One issue with seizure prediction studies is how to select

Table 3
The descriptions of each dataset in the Bonn University database [21].

Dataset	File name	Subject details	Description	Number of files (duration in seconds)
A	Z001.txt to Z100.txt	Five healthy subjects (normal)	Surface EEG recordings with eyes open	100 (23.6)
B	O001.txt to O100.txt		Surface EEG recordings with eyes closed	100 (23.6)
C	N001.txt to N100.txt	Five epilepsy patients	EEG readings of hippocampal formation in the hemisphere opposite the epileptogenic zone. Recorded during seizure-free periods.	100 (23.6)
D	F001.txt to F100.txt		EEG recordings of the epileptogenic zone. Recorded during seizure-free periods.	100 (23.6)
E	S001.txt to S100.txt		EEG recordings of epileptic seizure activity from the hippocampal focus.	100 (23.6)

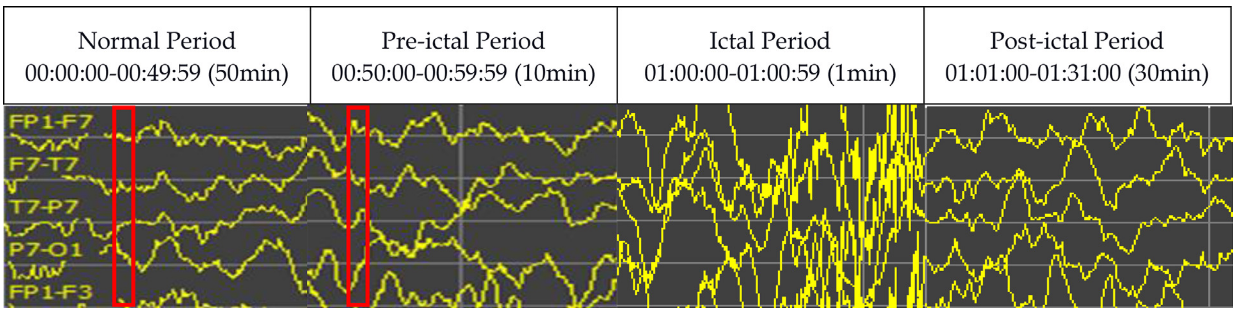

Fig. 2. An example of EEG signals sampling (Patient ID 1-1, channels of FP1-F7, F7-T7, T7-P7 and P7-O1). The red windows are the sampling signals (2.8 seconds of length in normal and pre-ictal periods). Yellow lines/waves over time show the activity from the EEG signals at the normal period (50 min), pre-ictal (10 min before the ictal period starts), ictal (1 min) and post-ictal (30 min after the ictal period) periods. The patient was an 11-year-old female. The recording rate is 256 Hz. The vertical scale is 50 µV.

pre-ictal EEG signal recording segments. The time between a prognostic symptom of a seizure and the start of a seizure is defined as the seizure prediction horizon (SPH), which has been reported to be between a few minutes and several hours. For both training and testing datasets, the SPH in this study is set at 10 minutes (2.8 seconds in duration). Therefore, pre-ictal samples are collected 10 minutes before seizure onsets. Data samples for a normal period (in 2.8-second duration and one-hour interval) are randomly selected in between pre-ictal and post-ictal periods (30 min after a seizure) (Fig. 2).

However, the SPH cannot be applied to the Bonn database because its ictal (dataset E) and non-ictal (dataset A-D) recordings are separated. Regarding the EEG signals from any specific area on the scalp, all electrode channels attached to the scalp are equally weighted, and EEG signals from all channels are evenly used.

3.3. Short time Fourier transformation (STFT)

STFTs are widely used for denoising time-dependent signals. The Fourier transform (FT) of function $f(x)$ is function $F(\omega)$, where:

$$F(\omega) = \int_{\infty}^{-\infty} f(x)e^{-i\omega t}dx \tag{1}$$

$$f(x) = 2\pi \int_{\infty}^{-\infty} F(\omega)e^{-i\omega t}d\omega \tag{2}$$

The fast Fourier transform (FFT) is a fast algorithm for computing the discrete FT. The FFT is a method for converting a signal's information into its frequency information where the time information cannot be recovered after the transformation. The STFT of a signal consists of the FFT of crossing windowed blocks of the signal (Fig. 3). The STFT, however, provides both information in a time-frequency domain as shown in Fig. 3. This study sets the window length as the FFT length, which is 10, and the overlap length is 5.

3.4. Synchroextracting transform (SET)

For a complex signal $s(t)$, which is the sum of n non-stationary modes, its expression is as follows [9]:

$$s(t) = \sum_{k=1}^{n} s_k(t) \ = \sum_{k=1}^{n} A(t)e^{i\varphi_k(t)} \tag{3}$$

where $\varphi'_{k+1}(t)$ - $\varphi'_k(t) > 2\Delta$, s_k, A_k, φ_k, denote the k_{th} mode, the corresponding instantaneous amplitude, and instantaneous phase, respectively. $\varphi_k{}'$ is the first-order derivative of φ_k and denotes instantaneous frequency; Δ is the frequency support of a window function. The STFT representation of $Ge(t, \omega)$ for the original signal $s(t)$, which forms the foundation of the SET, is displayed in the following form [9]:

$$Ge\ (t,\ \omega) \ = \ \sum_{k=1}^{n} A_k(t)\hat{g}\Big(\omega - \varphi'_k(t)\Big)e^{i\varphi_k(t)} \tag{4}$$

where $\hat{g}$ denotes the Fourier transform of the window function g, $g \in L_2(R)$. According to Eq. (4), the instantaneous frequency can be calculated by

$$\varphi'(t,\ \omega) \ = \ \sum_{k=1}^{n} \varphi' k(t,\ \omega) \ = -i\frac{\sigma_t G_e(t,\ \omega)}{G_e(t,\ \omega)} \tag{5}$$

Yu et al. (2017) developed an operator to only retain the time-frequency information from the STFT representation that is most related to the time-frequency characteristics of the target signal, which may remove the irrelevant interference and smeared time-frequency energy. The formula for the SET [9] is:

$$T_e(t,\ \omega) \ = \ G_e(t,\ \omega)\delta\Big(\omega - \varphi'(t,\ \omega)\Big) \tag{6}$$

where

$$\delta\Big(\omega - \varphi'(t,\omega)\Big) = \begin{cases} 1, & \omega = \varphi'(t,\omega) \\ 0, & else \end{cases} \tag{7}$$

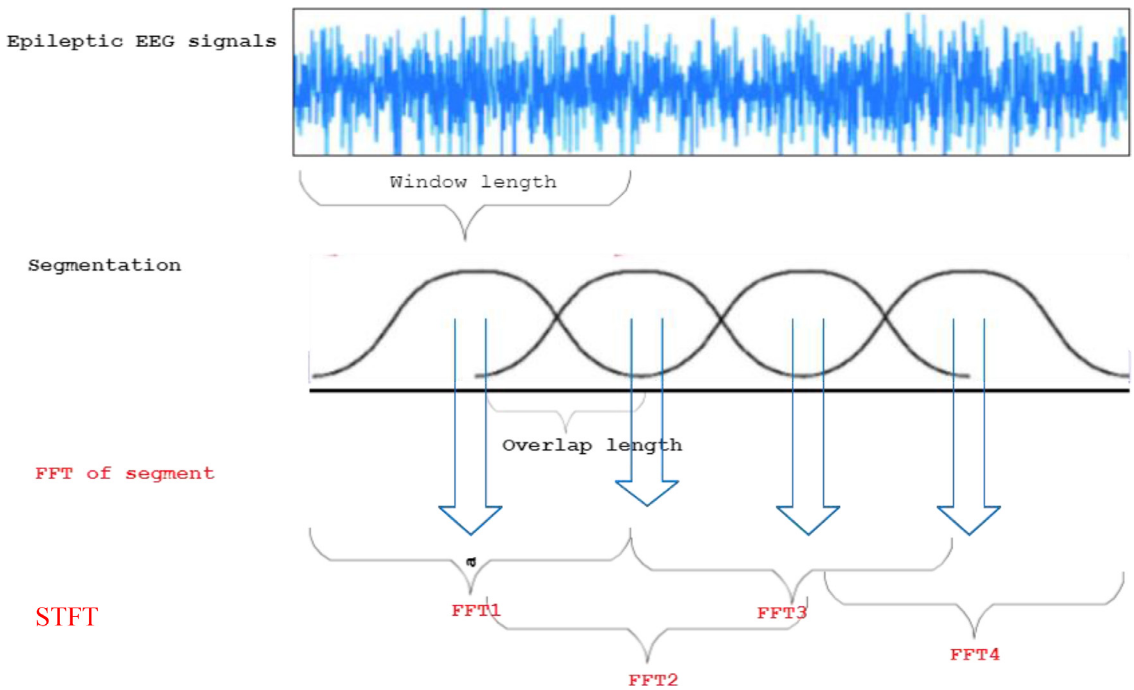

Fig. 3. The STFT of a signal consists of the FFT of crossing windowed blocks of the signal.

which is the synchroextracting operator (SEO). According to Eqs. (5) and (6), $Te(t, \omega)$ in SET can be deduced through Eq. (7) [9]:

$$Te(t,\omega)\big|_{\omega-\sum_{k=1}^{n}\varphi'_k(t)=0} = Ge(t,\ \omega)\big|_{\omega-\sum_{k=1}^{n}\varphi'_k(t)=0} \approx \sum_{k=1}^{n} A_k(t)\hat{g}(0)e^{i\varphi_k(t)} \tag{8}$$

In this way, a sharper time-frequency representation than the STFT can be obtained, and instantaneous frequency (IF) with a highly precise degree can be extracted.

3.5. Singular value decomposition of synchroextracting transform

The singular value decomposition (SVD) was developed by Eugenio Beltrami and Camille Jordan in 1873. An SVD is a matrix factorization into three matrices. It has intriguing algebraic properties and transmits essential geometrical and theoretical insights regarding linear transformations [22]. An SVD of an $M \times N$ matrix X, representing the SET values (Section 3.4) of the EEG signals is given by

$$X = USV^T \tag{9}$$

where $U(M \times M)$ and $V(N \times N)$ are orthonormal matrices, and S is an $M \times N$ diagonal matrix of singular values ($\sigma_{ij} = 0$ if $i \neq j$ and $\sigma_{11} \geq \sigma_{22} \geq \cdots \geq 0$). The columns of the orthonormal matrices U and V are called the left and right singular vectors, respectively. An important property of U and V is that they are orthogonal to one another. The singular values (σ_{ii}) represent the significance of singular vectors in the matrix's composition. In other words, singular vectors corresponding to larger singular values contain more information than other singular vectors regarding the content of patterns embedded in the matrix. In this study, 10 singular values (SET-SVD) are selected and employed.

3.6. Neural networks-based classification

Neural networks (NNs) process information using a mathematical or computational model, which is a network of simple processing elements capable of complex overall performance, as determined by the connections between processing elements and element parameters. This study applies two types of NNs, a multi-layer perceptron (MLP) and a convolutional neural network (CNN) to classify normal and pre-ictal stages of the STFT (Section 3.3) or SET-SVD (Section 3.5) of epileptic EEG signals.

3.6.1. Multi-layer perceptron (MLP)

The MLP, in this research, is learned using the backpropagation algorithm, where the errors of the hidden layer units are determined by back-propagating the errors of the output layer units. Its network consists of an input layer, a hidden layer, and an output layer. The activation function of the hidden layer is the sigmoid function, and its equation is given below.

$$S(x) = \frac{1}{1+e^{-x}} = \frac{e^x}{e^x+1} \tag{10}$$

Each connection between a node in the hidden layer and a node in the input layer has a weight. The backpropagation technique repeatedly modifies the weights of the links in the network to reduce the difference between the expected output vector of the network and the predicted output vector [23]. Each layer has a cost function, which is designated as follows and has its own least minimum error value:

$$C = cost\ \ (s,\ y) \tag{11}$$

where s is a predicted output value and y is an expected output value. The following describes the backpropagation algorithm to minimize the cost function:

1. The initial values of weight (w) and bias (b) are randomly chosen.
2. w and b are matrix representations of the weights and biases. Derivative of C in w or b can be calculated using partial derivatives of C in the individual weights or biases.
3. The termination condition is met once C is minimized to a threshold.

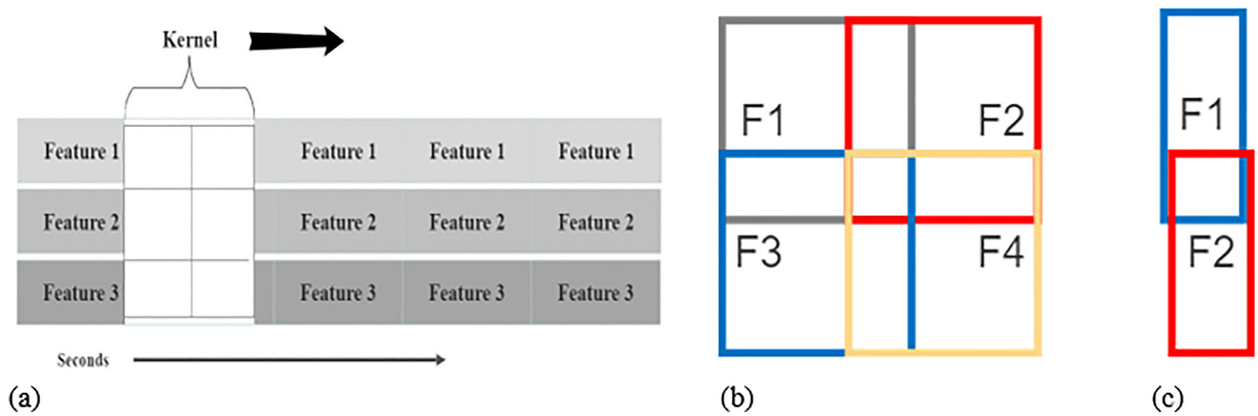

Fig. 4. (a) and (c) In 1D-CNN, the convolutional layer's kernel slides along one dimension; (b) In 2D-CNN, the convolutional layer's kernel moves along two dimensions.

Table 4
1D-CNN Structure Information.

1D-CNN Model structure layer	Kernel size	Activator	Output shape	Number of parameters
Convolutional 1D	2	ReLu	229×64	192
Dense	-	ReLu	229×16	1040
Max Pooling 1D	2		114×16	0
Flatten	-		1824	0
Dense	-	softmax	3	5475

Table 5
The confusion matrix of the classification performance of pre-ictal/normal period signals.

	True pre-ictal period	True normal period
Predicted pre-ictal period	A	B
Predicted normal period	C	D

Accuracy = (A + D) / (A + B + C + D).
Sensitivity = A / (A + C).
Specificity = D / (B + D).

3.6.2. 1-dimensional convolutional neural networks (1D-CNNs)

CNNs are a subclass of neural networks, which have at least one convolutional layer. Like MLPs, CNNs consist of an input layer and an output layer, and hidden layers. The main benefit of employing a CNN is that it can use its kernel to retrieve spatial information from the data. In 1D-CNN, the kernel slides along one dimension instead of two dimensions as shown in Fig. 4.

In this research, the first step of the 1D-CNN model is to rearrange the input data by creating one-dimensional vectors from each row of the input data. The input data dimension, 1430×230, is composed of 1430 steps with 230 features per step. And then, one convolutional layer, two dense layers, one max-pooling 1D layer and one flattened layer are added into the model structure. The convolutional layer consists of kernels that slide through the 1-dimensional data. The pooling layer (max-pooling layer in this study) is used to decrease the size of the convolutional layer outputs. This step involves sliding a window to take the maximum values in each window. The rectified linear unit activation function (ReLu) is used in the dense layer which is also called a fully connected layer. A summary of the proposed 1D-CNN model structure information is listed in Table 4. Kernel and max-pooling have a size of 2 and are used to decrease the size of neurons to 114×16.

4. Experimental results

The EEG signals are successfully decomposed by the SET-SVD and STFT, and they are classified into two groups of data, pre-ictal period and normal period. The scalograms illustrate that the SET method can generate more energy-concentrated TF results than the STFT (Fig. 5).

The efficiency of a seizure prediction algorithm (detecting pre-ictal signals) is determined by the accuracy, sensitivity, and specificity. Sensitivity is the percentage of the true pre-ictal prediction, and specificity is the percentage of the true normal period prediction (Table 5).

4.1. The CHB-MIT database

Table 6 presents the performance of the STFT and SET-SVD based on the MLP, and 1D-CNN classification tested using the 22 recordings in the CHB-MIT Scalp EEG Database. 720 datapoints (2.8 seconds of duration) are selected from each file. However, some files are excluded because interictal signals should be at least one hour ahead or after ictal signals. In addition, pre-ictal signals should be between suitable interictal signals. As the result, the total number of the data points is 5464800. 70% of the data are randomly selected for training (3825360 samples) and the remaining 30% are used for testing (1639440 samples). Fig. 6 illustrates the accuracy, specificity, and sensitivity of the related articles for comparisons.

In the MLP classification, the average accuracy by the SET-SVD is 94.73%, and that of STFT is 89.73%. The sensitivity and specificity of the MLP with the SET-SVD are higher (average 96.85% and 88.51%, respectively) than those with STFT (average 94.44% and 77.09%, respectively). The accuracy, sensitivity and specificity of the SET-SVD are improved by 5.0%, 2.41% and 11.42%, respectively. The average false positive rates (FPR) by the SET-SVD and STFT are 10.59% and 22.21%, respectively (average FPR = 1 – average specificity).

Based on the 1D-CNN, the average accuracy by the SET-SVD is 99.71%, and that of STFT is 91.59%. The sensitivity and specificity obtained by the 1D-CNN with the SET-SVD also show a higher rate (average 99.75 % and 99.56 %, respectively) than those with the STFT (average 93.51% and 85.65%, respectively). On average, the accuracy, sensitivity and specificity by the SET-SVD are increased by 8.12%, 6.24% and 13.91%, respectively. The average FPR by the SET-SVD and STFT are 0.44% and 14.35%, respectively.

Fig. 6 shows the comparison of the classification results by the proposed method and the methods from the reviewed studies that also applied the STFT and CNN to the CHB-MIT database. The p-values also confirm that the classification performances using the SET-SVD are significantly higher than those using the STFT (at $p < 0.05$) (Table 6).

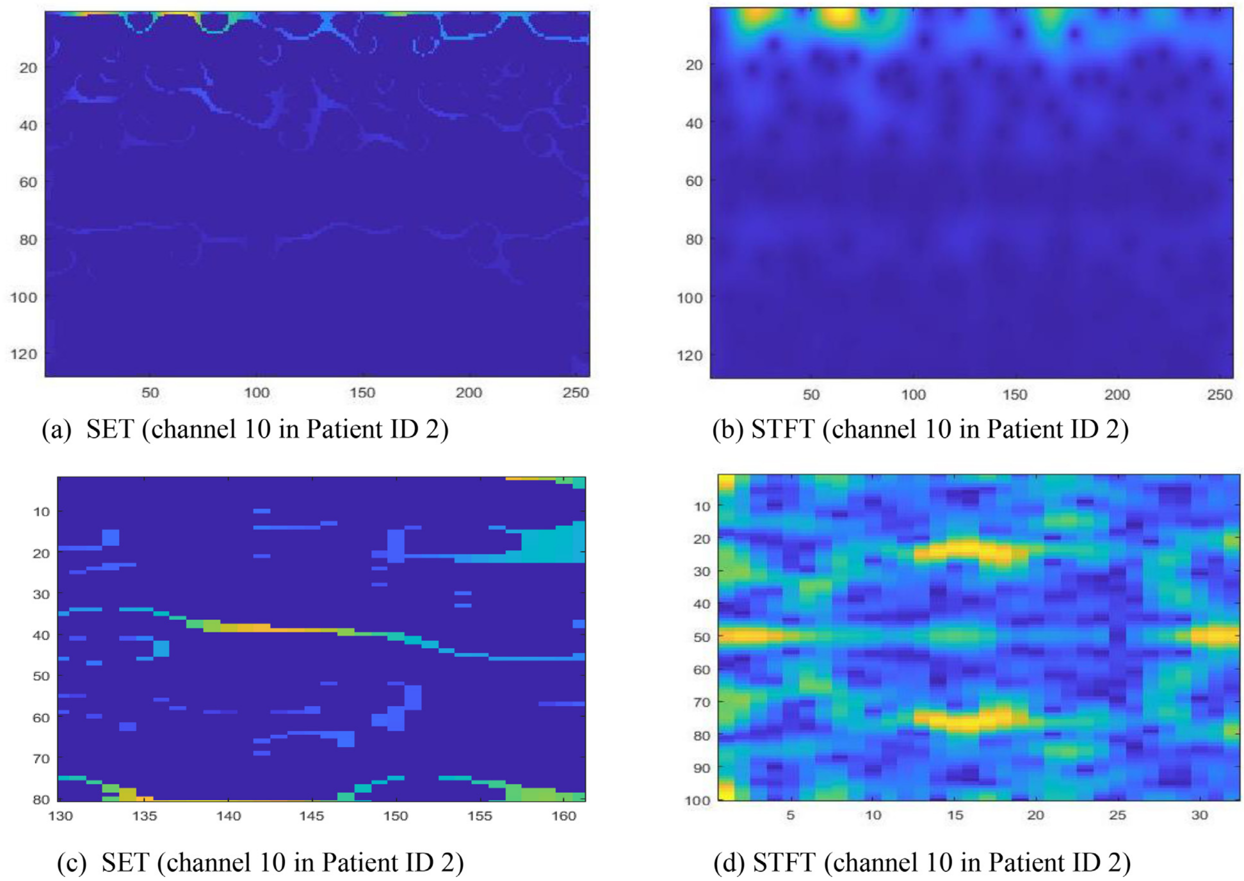

Fig. 5. Scalograms of the SET (a), (c) and STFT (b), (d) transform results. x-axis: time (1/256 seconds), y-axis: frequency (Hz). (c) and (d) are enlarged by zooming in of one sector of (a) and (b).

Table 6
The performance of the SET-SVD and STFT based on the MLP, and 1D-CNN classification tested on 22 recordings.

Patient ID	MLP						1D-CNN					
	Accuracy (%)		Sensitivity (%)		Specificity (%)		Accuracy (%)		Sensitivity (%)		Specificity (%)	
	SET-SVD	STFT	SET-SVD	STFT	SET-SVD	STFT	SET-SVD	STFT	SET-SVD	STFT	SET-SVD	STFT
1-1	93.84	93.99	87.47	96.98	91.17	87.35	100	98.9	100	99.08	100	98.54
2	99.59	96.89	99.87	97.19	98.62	95.45	100	98.71	100	99	100	97.7
3	98.36	89.19	99.26	95.26	93.94	70.04	99.83	92.9	99.84	95	99.76	86.16
4	97.01	83.87	98.95	99.77	91.07	28.8	99.75	99.1	99.77	100	99.67	95.76
5	93.5	88.83	97.8	92.17	76.77	72.41	99.85	88.93	99.84	92.01	99.89	68.15
6	97.11	86.99	96.94	93.67	97.35	77.67	99.69	89.32	99.74	90.97	99.62	87.22
7	91.99	89.78	95.22	89.38	89.91	91.2	99.61	88.89	99.63	93.06	99.54	76.43
8	98.05	96.34	98.76	96.83	96.79	95.52	99.8	98.34	99.95	98.25	99.55	98.51
9	97.78	91.45	99.15	99.81	94.89	52.63	99.66	96.27	99.81	97.4	99.01	90.48
10	89.74	84.2	97.18	94.81	75.56	64.58	99.87	82.41	99.88	85.61	99.85	75.51
11	98.26	90.68	99.35	94.17	93.06	73.26	99.65	89.71	99.77	93.01	99.08	73.26
12	98.52	96.5	99.39	97.17	97.21	95.6	99.63	97.2	99.54	96.62	99.77	97.92
14	95.93	81.8	86.93	95.28	95.28	71.01	99.75	79.81	99.72	86.67	99.81	65.55
15	89.41	76.36	95.26	86.39	86.39	45.04	99.38	84.63	99.47	89.06	99.26	77.69
16	94.62	77.06	82.83	87.33	87.33	62.96	99.57	77.60	99.65	82.85	99.39	65.55
17	94.33	94.37	98.17	81.79	81.79	83.46	99.46	95.15	99.74	95	98.61	95.65
18	92.77	94.04	95.96	84.58	84.58	87.64	99.72	91.98	99.83	93.32	99.33	86.79
19	96.62	99.04	98.84	88.16	88.16	100	99.89	100	99.87	100	100	100
20	92.98	94.73	93.37	84.05	84.05	100	100	98.89	100	100	100	96.14
1-2	87.3	85.28	93.55	80.25	80.25	60.92	99.58	83.55	99.57	88.45	99.59	69.32
21	96.49	94.56	94.24	87.04	87.04	95.49	99.73	95.53	99.79	97.06	99.53	91.49
22	96.11	88.11	91.39	95.72	95.72	85	99.17	87.18	99.18	84.86	99.15	89.57
Mean	**95.01**	**89.73**	**96.85**	**94.44**	**89.41**	**77.09**	**99.71**	**91.59**	**99.75**	**93.51**	**99.56**	**85.65**
standard deviation	**3.30**	**6.30**	**4.64**	**5.90**	**6.81**	**19.06**	**0.20**	**6.26**	**0.19**	**4.92**	**0.38**	**11.37**
standard error	**0.70**	**1.35**	**0.99**	**1.26**	**1.45**	**4.06**	**0.04**	**1.37**	**0.04**	**1.07**	**0.08**	**2.48**
p-value	**0.00**		**0.02**		**0.01**		**0.00**		**0.00**		**0.00**	

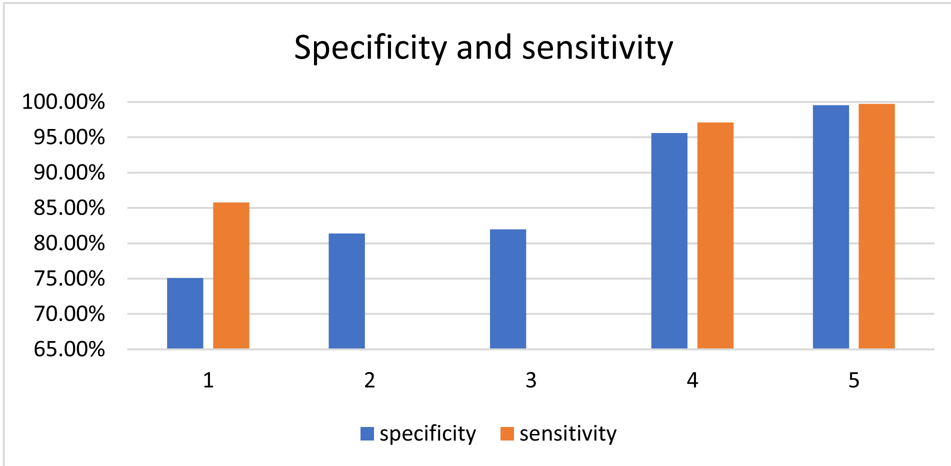

Fig. 6. Specificity and sensitivity of the related studies that applied the STFT and CNN with the CHB-MIT database. 1. Wang et al. (2021); 2. Truong et al. (2017); 3. Chen and Parhi (2021); 4. Sun et al. (2021); 5. The proposed method.

Table 7
The performance of the SET-SVD and STFT based on the MLP, and 1D-CNN classification tested using the Bonn University database.

	MLP						1D-CNN					
	Accuracy (%)		Sensitivity (%)		Specificity (%)		Accuracy (%)		Sensitivity (%)		Specificity (%)	
	SET-SVD	STFT	SET-SVD	STFT	SET-SVD	STFT	SET-SVD	STFT	SET-SVD	STFT	SET-SVD	STFT
A:B	100	98.70	100	97.37	100	100	100	98.45	100	98.23	100	98.62
A:C	100	99.57	100	99.12	100	100	100	100	100	100	100	100
A:D	100	98.26	100	96.49	100	100	99.78	99.22	100	100	99.57	98.59
B:C	100	99.13	100	100	100	98.28	100	99.61	100	99.15	100	100
B:D	100	99.78	100	100	100	99.57	100	100	100	100	100	100
AB:C	100	97.68	100	98.70	100	97.18	100	99.74	100	100	100	99.19
AB:D	100	99.42	100	99.13	100	99.57	100	100	100	100	100	100
C:D	100	99.35	100	99.12	100	99.57	100	98.84	100	100	100	97.67
Mean	**100**	**98.99**	**100**	**98.74**	**100**	**99.27**	**99.97**	**99.48**	**100**	**99.67**	**99.95**	**99.26**
standard deviation	**0.00**	**0.72**	**0.00**	**1.23**	**0.00**	**1.02**	**0.08**	**0.60**	**0.00**	**0.65**	**0.15**	**0.89**
standard error	**0.00**	**0.27**	**0.00**	**0.46**	**0.00**	**0.38**	**0.03**	**0.22**	**0.00**	**0.25**	**0.06**	**0.34**

In addition, the standard deviations (SDs) of both results from the 1D-CNN and MLP using the SET-SVD are meaningfully lower than those using the STFT. With the 1D-CNN, the SDs of accuracy, sensitivity and specificity from the results by the SET-SVD are lower by 6.06, 4.73 and 10.99 compared to those by the STFT, respectively, while with the MLP, they are lower by 3.00, 1.26 and 12.25, respectively).

4.2. The Bonn University database

The performances of the STFT and SET-SVD based on the MLP, and 1D-CNN classification tested on the Bonn EEG Database are presented in Table 7. 720 data points (4.15 seconds of duration) from each of 23 files per dataset (A, B, C or D) are analyzed. The total number of data points is 82800: Randomly selected, 70% of the data (57960 samples) were used for training, while the remaining 30% (24840 samples) were used for testing.

The classification outcomes for the SET-SVD sets exhibit nearly 100% accuracy, sensitivity, and specificity (99.95 – 100%). For classifying the STFT sets, the 1D-CNN (accuracy: 99.48%, sensitivity: 99.67%, specificity: 99.26%) is marginally superior to the MLP (accuracy: 98.99%, sensitivity: 98.74%, specificity: 99.27%). The SPH is not applicable to the Bonn database, but the accuracy performance obtained from various combinatory experiments suggests that the proposed method can predict seizures.

5. Discussion

There has been a paradoxical problem reported in signal analysis using the STFT. A longer window length results in a better frequency resolution but with a worse time resolution, while a shorter window length results in a better time resolution but would have a worse frequency resolution [24–28]. To improve the TF resolution as high as possible, one of the advanced post-processing methods, the SET, is successfully applied to the raw EEG signals, and it extracts useful information to predict the epileptic pre-seizure status. To the best of our knowledge, the SET has never been applied to analyze EEG signals for the prediction of pre-seizure status previously.

The SET represents only the TF information related to signal time-varying features [9]. It is clearer and more concentrated than the STFT (Fig. 5). Followed by the SVD, the SET can effectively describe the time-frequency characteristics of epileptic EEG signals. The experiments on the Bonn University database show that both the 1D-CNN and MLP can discriminate the SET-SVD sets with almost a zero-standard error. Tested on the CHB-MIT database, the average accuracy, sensitivity, and specificity by the 1D-CNN classification with the SET-SVD are 99.71%, 99.75% and 99.56%, respectively, which are 8.12%, 6.24% and 13.91% higher than the results by the STFT. Another classification method in this study, the MLP, also shows that the results by the SET-SVD are higher by 5.0%, 2.41% and 11.42% than those by the STFT in accuracy, sensitivity and specificity, respectively.

In addition, the SET shows more reliable test results than the STFT in this research. A high SD means that there is a large variance between the data and the mean. The SDs from the 1D-CNN results using the SET-SVD are lower than those by using the STFT (Table 6). The SDs of results from the MLP also confirm lower SDs from the SET-SVD, which indicates that the STFT is not as reliable as the SET-SVD. Da Silva et al. [29] showed that the STFT generates more significant data variability, resulting in less accurate classification performance than wavelet transform (WT) based methods. Oliveira et al. [30] also supported this conclusion using the results of variance, indicating less accuracy in terms of variability in data obtained from the analysis by the STFT. The STFT shows a large dispersion of individual values within the temporal window of processing and over time (successive windows), and consequently would result in larger measurement errors in dynamic situations, as suggested by Karlsson et al. [31].

This research also aims to reduce computational time for real-time seizure prediction while maintaining high accuracy in feature extraction and classification processes. EEG signals can be transformed from a wireless and/or portable EEG monitor to the necessary peripherals for acquisition alarms without sacrificing critical time [32]. The proposed 1D-CNN model is compact and has only one convolutional layer, which can reduce the processing time immensely. Recent studies [33–36] showed that the majority of 1D-CNN applications have employed a shallow structure that has one or two CNN layers and the number of parameters is less than 10000 (6707 in this research as shown in Table 4), while nearly all 2D-CNN applications have used architectures with more than one million parameters. Consequently, a 1D-CNN has a lower computational complexity than a 2D-CNN, and the testing time takes less than one second in this research.

6. Conclusion

In this research, the training and testing processing in the classification are patient-specific as the patterns of epileptic seizure occurrences are patient-dependent [20]. The experiments on two epileptic EEG databases (the Bonn and CHB-MIT) show that the SET-SVD has the capacity to extract more accurate information than the STFT. Especially, the SET-SVD with 1D-CNN can provide almost 100% of accuracy, sensitivity and specificity for predicting seizure status in both databases.

The performances by the STFT have a larger SD than those of the SET-SVD, which means that the STFT is less reliable. Using the STFT with the 1D-CNN, the specificity for Patient ID 5 in the CHB-MIT database is 68.15%, while the specificity for the same Patient ID by the SET-SVD with 1D-CNN achieved 99.89%. This type of weakness for the STFT is also found in other studies [29–31].

The effectiveness of the 1D-CNN in this research is promising. Compared with the MLP, the computational speed is much faster (more than 1000 times) and the accuracy is more than 10% higher. Although the experiments using a 2D or 3D-CNN were not conducted in this study, it was concluded from the literature review that the 1D-CNN would be faster (100 times lesser number of parameters) and more accurate (1-10%) than the 2D or 3D-CNN.

Declaration of Competing Interest

No conflict of interest is involved in this research.

Funding

This research received no external funding.

Institutional Review Board Statement

Ethical review and approval were waived for this study due to the secondary data used in this research. The data used are publicly available through the links below. https://scholar.google.com.au/scholar?q=Ali+Shoeb.+Application+of+Machine+Learning+to+Epileptic+Seizure+Onset+Detection+and+Treatment+PhD+Thesis+Massachusetts+Institute+of+Technology+September+2009&hl=en&as_sdt=0,5 (accessed on 23 October 2022). https://repositori.upf.edu/handle/10230/42894?show=full (accessed on 21 October 2020).

Informed Consent Statement

The data are from the CHB-MIT Scalp EEG Database and the Bonn University epilepsy database. They were publicly available online. The detailed information is in the links below. https://scholar.google.com.au/scholar?q=Ali+Shoeb+Application+of+Machine+Learning+to+Epileptic+Seizure+Onset+Detection+and+Treatment+PhD+Thesis+Massachusetts+Institute+of+Technology+September+2009&hl=en&as_sdt=0,5 (accessed on 23 October 2022). https://repositori.upf.edu/handle/10230/42894?show=full (accessed on 21 October 2020).

Data Availability Statement

The data and materials used in this study are available at the University of Southern Queensland under the research data management policy.

References

[1] J. Allen, Short term spectral analysis, synthesis, and modification by discrete Fourier transform, IEEE Transactions on Acoustics, Speech, and Signal Processing 25 (3) (1977) 235–238.
[2] P. Kumar, E. Foufoula-Georgiou, Wavelet analysis for geophysical applications, Reviews of geophysics 35 (4) (1997) 385–412.
[3] M. Qatmh, et al., Detection of epileptic seizure using discrete wavelet transform on gamma band and artificial neural network, in: 2021 14th International Conference on Developments in eSystems Engineering (DeSE), IEEE, 2021.
[4] R. Wilson, A.D. Calway, E.R. Pearson, A generalized wavelet transform for Fourier analysis: the multiresolution Fourier transform and its application to image and audio signal analysis, IEEE Transactions on Information Theory 38 (2) (1992) 674–690.
[5] P.J. Loughlin, J.W. Pitton, L.E. Atlas, Proper time-frequency energy distributions and the Heisenberg uncertainty principle, in: [1992]Proceedings of the IEEE-SP International Symposium on Time-Frequency and Time-Scale Analysis, IEEE, 1992.
[6] P. Busch, T. Heinonen, P. Lahti, Heisenberg's uncertainty principle, Physics Reports 452 (6) (2007) 155–176.
[7] E.P. Wigner, On the quantum correction for thermodynamic equilibrium, Physics Review 40 (1932) 749–759.
[8] P. Laplante, ACM SIGSOFT Software Engineering Notes, Heisenberg uncertainty 15 (5) (1990) 21–22.
[9] G. Yu, M. Yu, C. Xu, IEEE Transactions on Industrial Electronics, Synchroextracting transform 64 (10) (2017) 8042–8054.
[10] E. Sejdić, I. Djurović, J. Jiang, Time–frequency feature representation using energy concentration: An overview of recent advances, Digital signal processing 19 (1) (2009) 153–183.
[11] D. Gorur, et al., Sleep spindles detection using short time Fourier transform and neural networks, in: Proceedings of the 2002 International Joint Conference on Neural Networks. IJCNN'02 (Cat. No. 02CH37290), IEEE, 2002.
[12] N.D. Truong, et al., A generalised seizure prediction with convolutional neural networks for intracranial and scalp electroencephalogram data analysis, 2017. arXiv preprint arXiv: 1011.3382.
[13] R. Chen, K.K. Parhi, Seizure prediction using convolutional neural networks and sequence transformer networks, in: 2021 43rd Annual International Conference of the IEEE Engineering in Medicine & Biology Society (EMBC), IEEE, 2021.
[14] B. Sun, et al., Seizure prediction in scalp EEG based channel attention dual-input convolutional neural network, Physica A: Statistical Mechanics and its Applications 584 (2021) 126376.
[15] S. Kiranyaz, et al., Convolutional neural networks for patient-specific ECG classification, in: 2015 37th Annual International Conference of the IEEE Engineering in Medicine and Biology Society (EMBC), IEEE, 2015.
[16] S. Khalilpour, et al., Application of 1-D CNN to predict epileptic seizures using EEG records, in: 2020 6th International Conference on Web Research (ICWR), IEEE, 2020.

[17] B.P. Prathaban, R. Balasubramanian, Dynamic learning framework for epileptic seizure prediction using sparsity based EEG Reconstruction with Optimized CNN classifier, Expert Systems with Applications 170 (2021) 114533.
[18] Z. Wang, J. Yang, M. Sawan, A novel multi-scale dilated 3D CNN for epileptic seizure prediction, in: 2021 IEEE 3rd International Conference on Artificial Intelligence Circuits and Systems (AICAS), IEEE, 2021.
[19] M. Shahbazi, H. Aghajan, A generalizable model for seizure prediction based on deep learning using CNN-LSTM architecture, in: 2018 IEEE Global Conference on Signal and Information Processing (GlobalSIP), IEEE, 2018.
[20] J.S. Ra, T. Li, Y. Li, A novel permutation entropy-based EEG channel selection for improving epileptic seizure prediction, Sensors 21 (23) (2021) 7972.
[21] R.G. Andrzejak, et al., Indications of nonlinear deterministic and finite-dimensional structures in time series of brain electrical activity: Dependence on recording region and brain state, Physical Review E 64 (6) (2001) 061907.
[22] Chowning, S., *The Singular Value Decomposition*. 2020.
[23] D.E. Rumelhart, G.E. Hinton, R.J. Williams, Learning representations by back--propagating errors, nature 323 (6088) (1986) 533–536.
[24] A. Zabidi, et al., Short-time Fourier Transform analysis of EEG signal generated during imagined writing, in: 2012 International Conference on System Engineering and Technology (ICSET), IEEE, 2012.
[25] S.-H. Cho, G. Jang, S.-H. Kwon, Time-frequency analysis of power-quality distuvvvrbances via the Gabor–Wigner transform, IEEE transactions on power delivery 25 (1) (2009) 494–499.
[26] A. Chakraborty, D. Okaya, Frequency-time decomposition of seismic data using wavelet-based methods, Geophysics 60 (6) (1995) 1906–1916.
[27] H.R. Al Ghayab, et al., Epileptic seizures detection in EEGs blending frequency domain with information gain technique, Soft Computing 23 (1) (2019) 227–239.
[28] T. Nguyen-Ky, P. Wen, Y. Li, Consciousness and depth of anesthesia assessment based on Bayesian analysis of EEG signals, IEEE Transactions on Biomedical Engineering 60 (6) (2013) 1488–1498.
[29] R. Da Silva, et al., The comparison of wavelet-and Fourier-based electromyographic indices of back muscle fatigue during dynamic contractions: validity and reliability results, Electromyography and clinical neurophysiology 48 (3/4) (2008) 147.
[30] R.S. Oliveira, et al., Spectral analysis of electromyographic signal in supramaximal effort in cycle ergometer using Fourier and Wavelet transforms: a comparative study, Revista Andaluza de Medicina del Deporte 5 (2) (2012) 48–52.
[31] S. Karlsson, J. Yu, M. Akay, Time-frequency analysis of myoelectric signals during dynamic contractions: a comparative study, IEEE transactions on Biomedical Engineering 47 (2) (2000) 228–238.
[32] O. Kaziha, T. Bonny, in: *A convolutional neural network for seizure detection*. in *2020 Advances in Science and Engineering Technology International Conferences (ASET)*, IEEE, 2020.
[33] Y. Zhang, et al., Vibration-based structural state identification by a 1-dimensional convolutional neural network, Computer-Aided Civil and Infrastructure Engineering 34 (9) (2019) 822–839.
[34] O. Yildirim, et al., Automated detection of diabetic subject using pre-trained 2D-CNN models with frequency spectrum images extracted from heart rate signals, Computers in biology and medicine 113 (2019) 103387.
[35] J. Rahul, L.D. Sharma, Automatic cardiac arrhythmia classification based on hybrid 1-D CNN and Bi-LSTM model, Biocybernetics and Biomedical Engineering 42 (1) (2022) 312–324.
[36] M. Salem, S. Taheri, J.S. Yuan, ECG arrhythmia classification using transfer learning from 2-dimensional deep CNN features, in: 2018 IEEE biomedical circuits and systems conference (BioCAS), IEEE, 2018.